Available online at www.sciencedirect.com
ScienceDirect
Journal of the European Ceramic Society 31 (2011) 1473–1480
www.elsevier.com/locate/jeurceramsoc

Decomposition of $MgSiN_2$ in nitrogen atmosphere

Zoltán Lenčéš [a,*], Linda Pentráková [a], Monika Hrabalová [a], Pavol Šajgalík [a], Kiyoshi Hirao [b]

[a] *Institute of Inorganic Chemistry, Slovak Academy of Sciences, Dúbravská cesta 9, 845 36 Bratislava, Slovakia*
[b] *Advanced Manufacturing Processing Research Institute, National Institute of Advanced Industrial Science and Technology (AIST), Nagoya 463-8560, Japan*

Received 22 December 2010; received in revised form 7 February 2011; accepted 14 February 2011

Abstract

Magnesium silicon nitride $MgSiN_2$ was prepared by direct nitridation of $Si/Mg_2Si/Mg/Si_3N_4$ powder compact in a temperature range 1350–1420 °C. The thermal stability examination showed that $MgSiN_2$ is stable up to 1400 °C at 0.1 MPa N_2 pressure. The activation energy of decomposition of $MgSiN_2$ calculated from the temperature dependence of mass loss in the range of 1400–1650 °C is $\Delta H = 501$ kJ mol^{-1}. The time dependence and nitrogen pressure dependence of $MgSiN_2$ decomposition was also investigated at constant temperature. $MgSiN_2$ is stable at 1560 °C in 0.6 MPa nitrogen atmosphere. Using these experimental data together with the heat capacity published in a literature the Gibbs energy of formation of $MgSiN_2$ was calculated in a temperature range 25–2200 °C.

Keywords: Nitrides; Decomposition; $MgSiN_2$; Enthalpy

1. Introduction

In the past two decades great attention has been given to the development of nitride-based ceramic materials with high thermal conductivity. The most promising results have been achieved for AlN and Si_3N_4 with thermal conductivity 260 and 162 W(m K)$^{-1}$, respectively.[1,2] Except of special processing methods like seeding, tape casting, or extrusion with a goal to obtain highly oriented microstructure, the main attention of research groups is focused on the grain boundary chemistry. It was confirmed that the lattice oxygen has a deleterious effect on thermal conductivity.[3] For that reason rare-earth oxides (e.g. Y_2O_3, Yb_2O_3, Nd_2O_3, etc.) or nonoxide sintering additives like fluorides, nitrides, or borides are used for the sintering of AlN or Si_3N_4 with high thermal conductivity.[4] Hayashi et al.[5] reported thermal conductivity over 140 W(m K)$^{-1}$ for sintered Si_3N_4, using Yb_2O_3, MgO and $MgSiN_2$ as sintering additives. Besides MgO also $MgSiN_2$ was used as a supplier of Mg^{2+} ions, which decreased the melting point of silicate glass, but without increasing the oxygen content in the liquid phase. During thermal annealing at 1900 °C and 0.9 MPa nitrogen pressure $MgSiN_2$ decomposed to Mg and N_2 vapours, and to solid Si_3N_4. Magnesium can pick up some oxygen from the silicate melt, evaporates also in a form of MgO gas and decreases the total oxygen content in the sintered body. This "cleaning effect" resulted in higher thermal conductivity. The main disadvantage of the applied method was the long annealing time at very high temperature.

The conditions for the evaporation of MgO from partly sintered Si_3N_4 body were already published,[6] however, concerning the decomposition of $MgSiN_2$ there is a lack of data. In earlier works it was reported that $MgSiN_2$ is stable at 1500 °C in nitrogen atmosphere and the approximate Gibbs free energy of $MgSiN_2$ can be described by the following equation[7]:

$$G(MgSiN_2) = -165,000 + 75.96T \quad \text{(J/g-atom)}.$$

On the other hand Uchida et al. observed the decomposition of $MgSiN_2$ to α-Si_3N_4 and β-Si_3N_4 at temperatures exceeding 1400 °C.[8] Groen et al. reported the decomposition of $MgSiN_2$ at 1550 °C in welded molybdenum vessel in argon ambient.[9] They found bubbles inside the sintered pellets probably due to the evaporation of Mg during sintering. When $MgSiN_2$ powder bed was used, the decomposition was successfully suppressed. These results suggest that the decomposition of $MgSiN_2$ starts at temperatures 1400–1500 °C in nitrogen atmosphere. Because the temperature range is relatively wide and the nitrogen pressure was also different, more detailed study is necessary. The ther-

* Corresponding author. Tel.: +421 259410408; fax: +421 259410444.
E-mail address: Zoltan.Lences@savba.sk (Z. Lenčéš).

0955-2219/$ – see front matter © 2011 Elsevier Ltd. All rights reserved.
doi:10.1016/j.jeurceramsoc.2011.02.023

mal stability data are also important for the sintering process above 1500 °C, when $MgSiN_2$ should remain in the product. Composites on the base of $MgSiN_2$ and Si_3N_4 with promising mechanical properties have been prepared by sintering at temperatures 1500–1650 °C and in nitrogen overpressure.[10–14] However, after sintering at these temperatures under 0.1 MPa N_2 atmosphere remarkable mass loss of 10–15% has been observed.[11]

The knowledge of thermal stability of $MgSiN_2$ is important also for the synthesis of long lasting phosphors, e.g. europium-doped $MgSiN_2$.[15–17]

The aim of this work was to study the decomposition of $MgSiN_2$ powder compacts in a temperature range 1400–1650 °C and 0.1 MPa nitrogen atmosphere. Some additional experiments in higher nitrogen pressure $p(N_2) \leq 0.8$ MPa and at constant temperature have been also carried out.

2. Experimental

$MgSiN_2$ powder was prepared from the mixture of Mg_2Si (99%, Kojundo Chem. Lab., Japan), α-Si_3N_4 (grade E-05, Ube Industries Ltd., Japan), Si (99.9%, Kojundo Chem. Lab., Japan), and Mg (grade Mg-100, Yamaishi Metal Co., Japan). The details of powder preparation are described elsewhere.[18] Briefly, stepwise heating was applied up to the final temperature of nitridation at 1380 °C and 0.1 MPa N_2 atmosphere. XRD analysis showed a single-phase $MgSiN_2$. The powder contained 33.36 wt% nitrogen and 0.62 wt% oxygen, determined by N/O analyzer (model TC-436, LECO Co., St. Joseph, MI).

The decomposition experiments were carried out in high purity nitrogen atmosphere (grade 5N) under conditions similar to the real sintering process. Differential thermal analysis (DTA) and thermogravimetry (TG) were conducted using TG-DTA apparatus (Thermo Plus TG 8120, Rigaku, Japan) with Al_2O_3 sample holders applying a constant heating rate of 5 °C min^{-1} in flowing nitrogen atmosphere (80 cm^3 min^{-1}) up to 1400 °C.

The decomposition experiments of $MgSiN_2$ were carried out in the temperature range of 1400–1650 °C on larger pellets (16 mm diameter, 2 mm height), prepared from the above mentioned $MgSiN_2$ powder by die-pressing (70 MPa) and cold-isostatic pressing (400 MPa). The samples were placed into a BN crucible on $MgSiN_2$ pin-holders and annealed in alumina tube furnace ($\phi = 80$ mm, Motoyama Ltd., Japan) with a heating rate of 3 °C min^{-1} and a holding time for 2 h at the final temperature. The nitrogen gas flow was maintained at 1.5 L min^{-1} during the measurements.

Decomposition experiments were carried out also in graphite gas–pressure furnace with nitrogen overpressure up to 0.8 MPa. The nitrogen gas flow was 1.5 L min^{-1}. The sample was placed into BN crucible and then to the larger graphite crucible. The inner walls of graphite crucible were coated with BN to decrease the carbon activity. In the graphite resistance furnace the temperature was controlled by pyrometer. Because the crucibles shielded the samples from heat radiation, the temperature was re-calibrated after the experiments: hole was drilled into the used crucibles, thermocouple was inserted and the real temperature near the sample was measured.

Table 1
Mass loss $\Delta m/m_0$ of $MgSiN_2$ samples after heat treatment at particular temperatures for 2 h in 0.1 MPa nitrogen atmosphere.

Temperature (°C)	1400	1450	1500	1550	1600	1650
$\Delta m/m_0$ (wt%)	−0.4	−1.9	−4.5	−13.2	−22.9	−44.3

The phase composition of heat treated samples was analysed by X-ray diffraction (XRD) measurements using Cu Kα radiation (RINT2500, Rigaku Co., Japan) with a scanning rate 2 °C min^{-1} and step 0.010° in the range $2\theta \in \langle 20°;70° \rangle$. The microstructural observation and elemental analysis were carried out by field-emission scanning electron microscope (JEOL JSM-6330F, Japan), equipped with energy-dispersive spectrometer (EDS, JEOL JED-2140, Japan).

3. Results and discussion

3.1. Thermal stability

The DTA-TG measurement did not show any significant decomposition of $MgSiN_2$ up to 1390 °C in 0.1 MPa nitrogen atmosphere. There was a mass loss of 0.67 wt% up to 600 °C, due to the removal of absorbed humidity from the samples (pre-annealed at 110 °C). Similarly, sample annealed up to 1300 °C in alumina tube furnace and 0.1 MPa nitrogen pressure showed mass loss of 0.72 wt%. Based on the results of these experiments, all the measured mass loss data were corrected by the systematic error of 0.7 wt%. The DTA-TG measurement showed slight weight loss starting at 1331 °C, but it was only 0.2 wt% in total measured on 58.5 mg sample in the range of 700–1390 °C.

The results of decomposition measurements of $MgSiN_2$ at temperatures above 1400 °C in alumina tube furnace are summarised in Table 1. The decomposition of $MgSiN_2$ starts at ~1400 °C in flowing nitrogen atmosphere. XRD measurement showed that after annealing of $MgSiN_2$ at this temperature a small amount of α-Si_3N_4 was formed in the product by the decomposition of ternary nitride. It was reported that $MgSiN_2$ decomposes after annealing in vacuum (1.3 Pa) at temperatures from 1000 °C to 1400 °C into Si_3N_4 and Mg_3N_2.[19] However, in the temperature range from 1400 °C to 1650 °C the proposed reaction of decomposition is the following:

$$3MgSiN_2(s) = 3Mg(g) + N_2(g) + Si_3N_4(s) \quad (1)$$

because Mg_3N_2 decomposes at these temperatures.[20] The theoretical mass loss according to reaction (1) is 41.8 wt%. Sample annealed at 1650 °C for 2 h had a mass loss of 44.3 wt% (Table 1). This difference indicates that Si_3N_4 should partly decompose already at 1650 °C. The decomposition of $MgSiN_2$ above 1650 °C can be expressed by reaction:

$$3MgSiN_2(s) = 3Mg(g) + 3xSi(l) + (1-x)Si_3N_4(s) + (1+2x)N_2(g) \quad (2)$$

where $x \in \langle 0; 1 \rangle$. According to JANAF thermochemical tables the decomposition temperature of Si_3N_4 is 1878 °C in 0.1 MPa

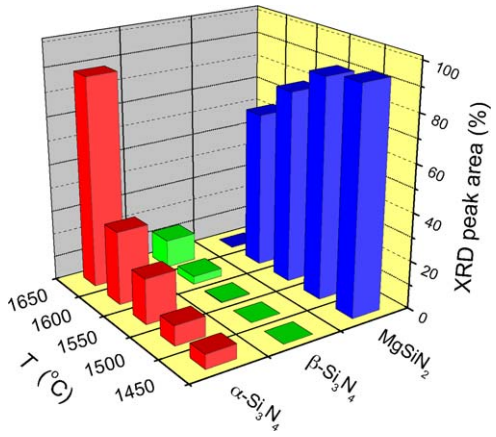

Fig. 1. The phase composition of $MgSiN_2$ samples heat treated for 2 h in 0.1 MPa nitrogen atmosphere at different temperatures.

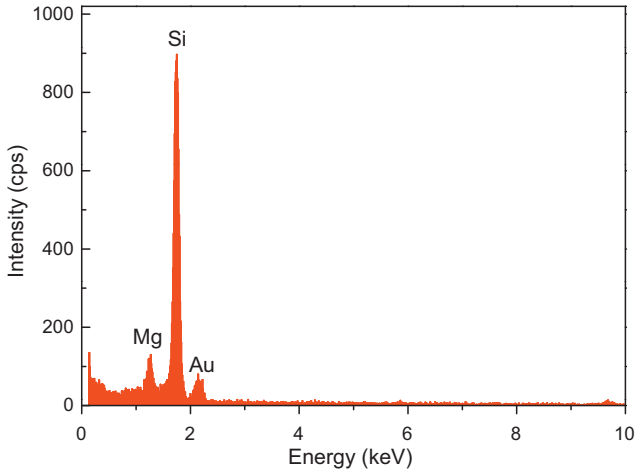

Fig. 3. EDX analysis of rod-like β-Si_3N_4 grains formed by decomposition of $MgSiN_2$ showing the presence of magnesium.

nitrogen atmosphere.[20] However, in practice the decomposition of Si_3N_4 is enhanced by impurities like carbon, oxygen, etc.[21,22] The starting $MgSiN_2$ powder used in this work contained 0.62 wt% oxygen, which is partly removed during annealing in a form of SiO(g) and MgO(g), resulting in ~1.7 wt% mass loss. Even with this contribution, the weight loss should not exceed 43.5 wt% (Table 1), if Si_3N_4 does not decompose at 1650 °C. All the results indicate the decomposition of Si_3N_4. Moreover, the product had a brownish colour after heat treatment at 1650 °C, while samples annealed at lower temperatures were white. It suggests to the presence of free silicon, however, it was bellow the detection limit of XRD analysis. Most probably the magnesium vapour catalysed the decomposition of Si_3N_4 (see Eq. (2)) at this relatively low temperature. David et al. reported that magnesium can reduce Si_3N_4 already at 1000 °C.[23]

The phase composition of annealed samples is shown in Fig. 1. α-Si_3N_4 is the major decomposition product. β-Si_3N_4 was formed at 1550 °C as a minor phase, and its content increased with increasing temperature. The $MgSiN_2$ content in sample annealed at 1650 °C for 2 h in 0.1 MPa nitrogen atmosphere was close to the lowest detection limit of XRD analysis.

The microstructure evolution of heat treated samples is shown in Fig. 2a–e. The powder agglomerates were partly sintered at 1400 °C, and at 1500 °C channels were formed between the grains by the evaporation of decomposition products. At 1650 °C rod-like β-Si_3N_4 grains were formed, however the EDS analysis of these grains shows the presence of small amount of magnesium (Fig. 3). Very often porous channels were observed within the elongated grains formed above 1600 °C (Fig. 2e).

The activation energy for decomposition of $MgSiN_2$ was estimated from the mass loss data shown in Fig. 4. The mass change as a function of temperature can be expressed by the approximate equation[24]:

$$\frac{\Delta m}{m_0} \approx \frac{ART^2}{\Delta H} \exp\left(-\frac{\Delta H}{RT}\right) \quad (3)$$

where m is the mass of sample, A the pre-exponential factor, R the gas constant and ΔH is the change of enthalpy.

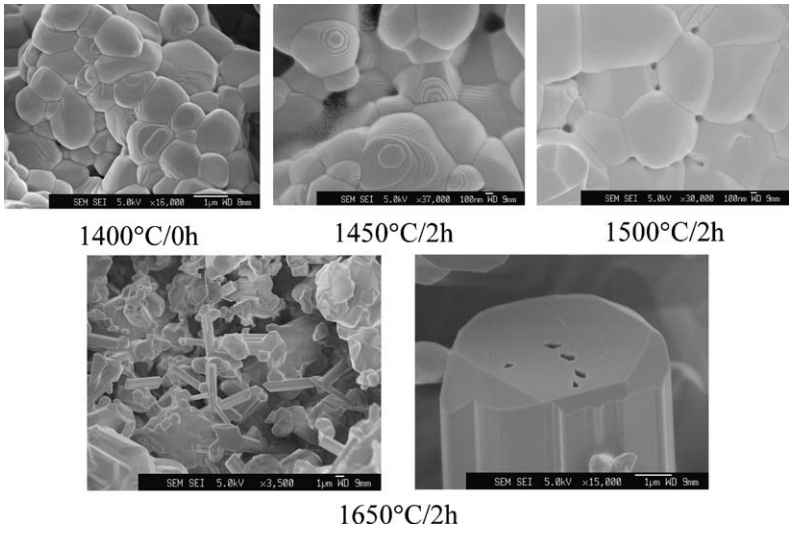

Fig. 2. Microstructure evolution of heat treated $MgSiN_2$ samples.

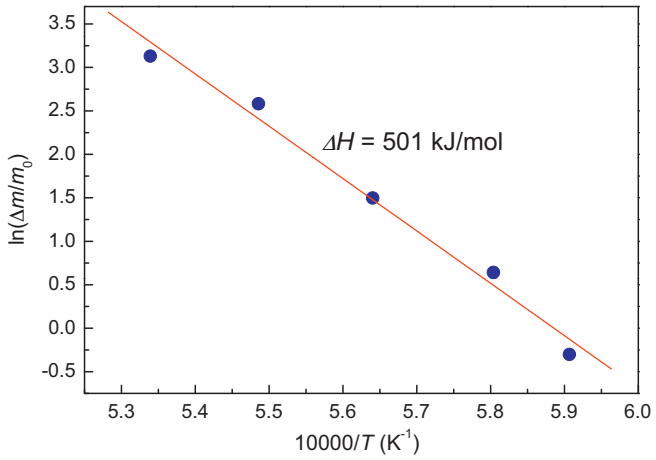

Fig. 4. The mass change as a function of temperature. The activation energy of decomposition $\Delta H = 501\ \mathrm{kJ\ mol^{-1}}$ was determined from the plot of $\ln(\Delta m/m_0)$ as a function of $1/T$.

The activation energy of decomposition $\Delta H = 500.7\ \mathrm{kJ\ mol^{-1}}$ was determined from the plot of $\ln(\Delta m/m_0)$ as a function of $1/T$. It should be noted that the enthalpy of formation $\Delta_f H^{\circ}_{298}$ for Mg_3N_2 and α-Si_3N_4 is $-461.08\ \mathrm{kJ\ mol^{-1}}$ and $-744.75\ \mathrm{kJ\ mol^{-1}}$, respectively.[20] Recent calorimetric studies gave enthalpies of formation $-828.9\ \mathrm{kJ\ mol^{-1}}$,[25,26] or $-850.9\ \mathrm{kJ\ mol^{-1}}$ for α-Si_3N_4.[22]

The time dependence of isothermal decomposition of $MgSiN_2$ was measured in alumina tube furnace at 1600 °C and 0.1 MPa nitrogen pressure. The results are shown in Fig. 5, where α is the fractional decomposition of $MgSiN_2$. The computation of the kinetic parameters was based on the Arrhenius equation applied to solid-state reactions, although its applicability is still the subject of debate. The decomposition data did not follow any of the mathematical models for solid-state reactions summarised by Šesták and Berggren for the whole time interval.[27] The initial decomposition is localised at the surface, and with the extent of reaction most probably the reaction mechanism is changed. For this reason the initial stages of decomposition ($t < 10$ min) were fitted to the first order reaction mechanism $d\alpha/dt = k(1-\alpha)$,[28]

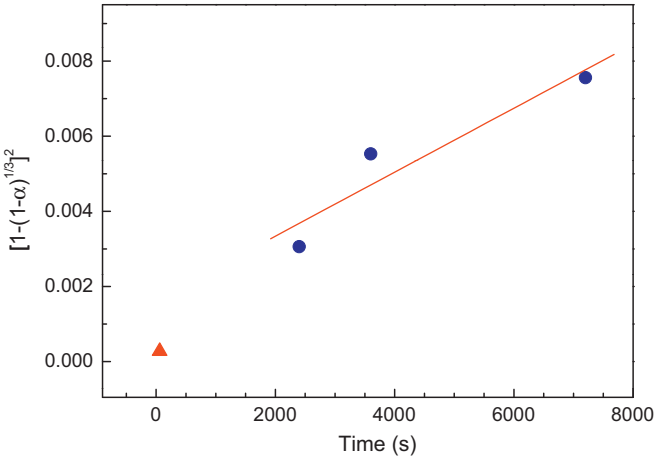

Fig. 5. The time dependence of isothermal decomposition of $MgSiN_2$ at 1600 °C and 0.1 MPa nitrogen pressure.

Table 2
Influence of nitrogen pressure on the mass loss (decomposition) of $MgSiN_2$ at 1560 °C and holding time for 2 h.

N_2 pressure (MPa)	0.1	0.3	0.4	0.5	0.6	0.8
Mass loss (wt%)	14.53	4.71	1.17	0.95	0.06	0.04

while for time $t > 30$ min the Jander's kinetic model has been applied[29]:

$$[1-(1-a)^{1/3}]^2 = \left(\frac{KD}{r^2}\right)\cdot t = k_J \cdot t \quad (4)$$

Coefficient K is determined by the chemical potential difference for the species diffusing across the reaction layer, D is the diffusion constant and r the radius of spherical particles. The linear fit of decomposition data in Fig. 5 yields the rate constant $k_J = 8.51 \times 10^{-7}\ \mathrm{s^{-1}}$ in Eq. (4). The temperature dependence of the reaction-rate constant follows also the Arrhenius equation $k_A = A\exp(-\Delta H/RT)$. Substituting the activation energy of decomposition $\Delta H = 500.7\ \mathrm{kJ\ mol^{-1}}$ (Fig. 4) and temperature 1873 K yields $k_A = A \times 1.09 \times 10^{-14}\ \mathrm{s^{-1}}$. The pre-exponential factor $A = 7.82 \times 10^7$ results from $k_J = k_A$. Finally, the temperature dependence of reaction-rate constant for time $t > 30$ min can be expressed by:

$$k = 7.82 \times 10^7 \exp\left(\frac{-60,224}{T}\right)\ \mathrm{s^{-1}} \quad (5)$$

It should be pointed out that the simplifications limit the range over which Eq. (5) adequately predicts the reaction rates. Jander's Eq. (4) is valid only for small reaction thickness and the molar volume change between the reactants and products was neglected; $V_{m,298}(MgSiN_2) = 2.562 \times 10^{-5}\ \mathrm{m^3\ mol^{-1}}$, $V_{m,298}(Si_3N_4) = 4.381 \times 10^{-5}\ \mathrm{m^3\ mol^{-1}}$.[30] However, due to the lack of the kinetic parameters determined by more precise methods, Eq. (5) gives at least a rough estimation of the decomposition rate of $MgSiN_2$.

The influence of nitrogen pressure on the decomposition of $MgSiN_2$ was investigated in graphite resistance gas pressure furnace at 1560 °C with a holding time of 2 h and nitrogen gas flow $1.5\ \mathrm{L\ min^{-1}}$. The results are summarised in Table 2 and shows that $MgSiN_2$ is stable at 1560 °C under 0.6 MPa nitrogen pressure.

Table 3
The coefficients and statistics used for describing the isobaric heat capacity C°_P (see Eq. (6)) of $MgSiN_2$ in a temperature range (300–1600) K from data in Bruls et al.[30]

Coefficient		Statistics	
a ($\mathrm{J\ K^{-1}\ mol^{-1}}$)	100.855	Data points	14
b ($\mathrm{J\ K^{-2}\ mol^{-1}}$)	1.542×10^{-3}	χ^2	4.28×10^{-3}
c ($\mathrm{J\ K\ mol^{-1}}$)	−6,243,640		
d ($\mathrm{J\ K^{-3}\ mol^{-1}}$)	-5.812×10^{-8}		
f ($\mathrm{J\ K^{2}\ mol^{-1}}$)	80,3546,405		

Table 4
Calculated thermodynamic properties of $MgSiN_2$ (reference temperature 298.15 K, standard state pressure 0.1 MPa).

T (K)	C_P° (exp.)[a] ($J\,K^{-1}\,mol^{-1}$)	C_P° (calc.)[b] ($J\,K^{-1}\,mol^{-1}$)	S° ($J\,K^{-1}\,mol^{-1}$)	$(G^\circ - H_{298}^\circ)/T$ ($J\,K^{-1}\,mol^{-1}$)	$H^\circ - H_{298}^\circ$ ($kJ\,mol^{-1}$)	$\Delta_f H^\circ$ ($kJ\,mol^{-1}$)	$\Delta_f G^\circ$ ($kJ\,mol^{-1}$)
298	61.34	61.365	44.140	−44.140	0	−542.610	−483.320
300	61.71	61.699	44.552	−44.141	0.123	−542.624	−482.922
400	75.04	74.994	64.277	−46.748	7.012	−543.329	−462.888
500	83.07	83.064	81.952	−52.057	14.948	−543.277	−442.773
600	88.08	88.135	97.578	−58.368	23.526	−542.825	−422.709
700	91.45	91.505	111.434	−64.979	32.518	−542.196	−402.738
800	93.85	93.864	123.815	−71.573	41.793	−541.527	−382.860
900	95.63	95.588	134.975	−78.008	51.270	−540.908	−363.066
923		95.920	137.392	−79.458	53.473	−540.793	−358.582
1000	96.99	96.897	145.117	−84.220	60.897	−549.010	−342.645
1100		97.922	154.402	−90.184	70.640	−548.629	−322.003
1200	98.88	98.748	162.959	−95.897	80.475	−548.273	−301.418
1300		99.430	170.891	−101.364	90.385	−547.928	−280.860
1366	100.05	99.819	175.825	−104.844	96.961	−547.723	−267.358
1400		100.004	178.281	−106.597	100.358	−675.011	−257.161
1500	100.72	100.497	185.198	−111.609	110.383	−673.358	−227.374
1600		100.928	191.698	−116.414	120.455	−671.729	−197.694
1685		101.254	196.931	−120.345	129.048	−670.368	−171.708
1700		101.308	197.829	−121.024	130.567	−720.306	−162.199
1800		101.649	203.629	−125.454	140.715	−718.505	−129.714
1900		101.959	209.133	−129.714	150.896	−716.692	−97.334
2000		102.242	214.370	−133.817	161.106	−714.870	−65.053
2100		102.504	219.365	−137.773	171.344	−713.035	−32.861
2200		102.747	224.139	−141.591	181.606	−711.191	−6.345
2300		102.975	228.712	−145.280	191.893	−709.338	25.648
2400		103.191	233.099	−148.849	202.201	−707.475	57.568
2500		103.394	237.316	-152.303	212.53	−705.603	89.403

[a] Data from Bruls et al.[30]
[b] Calculated from Eq. (6) and Table 3.

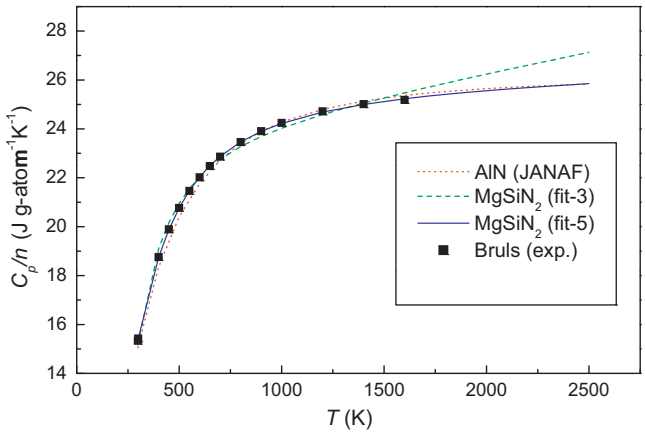

Fig. 6. The calculated and experimental heat capacities of $MgSiN_2$ and AlN.

3.2. Estimation of $\Delta_f G^\circ(MgSiN_2)$

In order to estimate the Gibbs energy of formation for $MgSiN_2$, the thermodynamic functions S_T° and $H_T^\circ - H_{298}^\circ$ were calculated from the heat capacity of $MgSiN_2$ at constant pressure C_P° published by Bruls et al.[30,31] The heat capacity data were obtained by DSC and adiabatic calorimeter measurements. We have fitted the heat capacity values in the temperature range (250–1600) K using the extended Maier–Kelley polynomial:

$$C_P^\circ = a + b \cdot T + c \cdot T^{-2} + d \cdot T^2 + f \cdot T^{-3} \quad (6)$$

The calculated coefficients are listed in Table 3 and the experimental data together with fitted curves are shown in Fig. 6. The 5-parameter polynomial (Eq. (6)) fits better the data compared to the basic Maier–Kelley polynomial ($C_P^\circ = a + b \cdot T + c \cdot T^{-2}$), especially at higher temperatures. The heat capacities of well characterised AlN are also plotted in Fig. 6. Owing to the same wurtzite-like structure of AlN and $MgSiN_2$, about the same average atomic mass and volume per atom, about the same sound velocity and Debye temperature, also the heat capacity per mole atoms (C_P/n, where n is the number of atoms in the substance) should be nearly the same.[30] Fig. 6 shows a good agreement of C_P/n for both compounds.

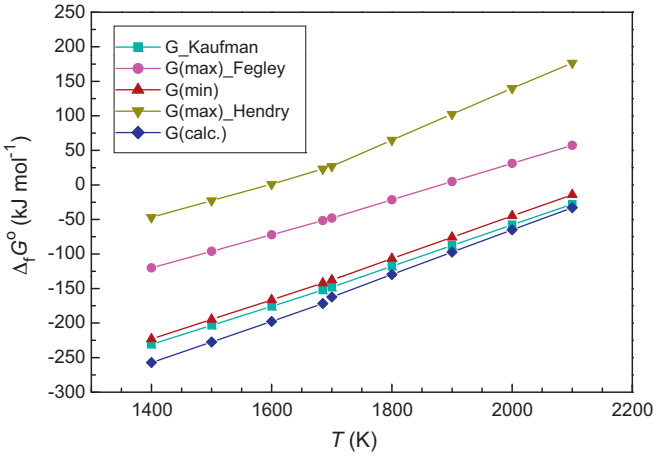

Fig. 7. Estimation of the minimum and maximum values of the $\Delta_f G^\circ$ ($MgSiN_2$) from Eqs. (14) and (15).

The relative enthalpy $H_T^\circ - H_{298}^\circ$ and entropy S_T° functions were obtained by numerical integration of C_P° and C_P°/T functions. $S_{298}^\circ = 44.14\,\mathrm{J\,mol^{-1}\,K^{-1}}$ was adopted from Bruls et al.[31] The enthalpy of formation of $MgSiN_2$ from elements was calculated using the Kirchhoff's law:

$$\Delta_f H_{298}^\circ = \Delta_f H_{298}^\circ + [H_{298}^\circ - H_0^\circ]_c - \sum [H_{298}^\circ - H_0^\circ]_e \quad (7)$$

where indices c and e denotes compound ($MgSiN_2$) and elements, respectively. The thermodynamic functions $H_{298}^\circ - H_0^\circ$ of elements were taken from NIST-JANAF tables,[20] $H_0^\circ(MgSiN_2) = -534\,\mathrm{kJ\,mol^{-1}}$ and $(H_{298}^\circ - H_0^\circ)_{MgSiN_2} = 8.278\,\mathrm{kJ\ mol^{-1}}$ from Bruls et al.[31] This dataset yielded the enthalpy of formation of $MgSiN_2$ at 298.15 K: $\Delta_f H_{298}^\circ = -542.6\,\mathrm{kJ\ mol^{-1}}$. The enthalpy and the Gibbs free energy of formation for $MgSiN_2$ were calculated using the following equations[20]:

$$\Delta_f H_T^\circ = \Delta_f H_{298}^\circ + [H_T^\circ - H_{298}^\circ]_c - \sum [H_T^\circ - H_{298}^\circ]_e \quad (8)$$

$$\Delta_f G_T^\circ = \Delta_f H_T^\circ - T[(S_T^\circ)_c - \sum (S_T^\circ)_e] \quad (9)$$

The enthalpies and entropies of the elements in reference state Mg(*ref*), Si(*ref*) and N_2(*ref*) were taken from NIST-JANAF tables.[20] The calculated thermodynamic functions in the temperature range of (298–2500) K are listed in Table 4.

The linear fit of the calculated Gibbs free energy of formation for $MgSiN_2$ in the temperature range of 1400–1680 K (above the boiling point of magnesium $T_{b,Mg} = 1366$ K) follows the equation:

$$\Delta_f G_T^\circ/(\mathrm{kJ\ mol^{-1}}) = -676.17 + 0.299T/\mathrm{K} \quad (10)$$

At temperatures above the melting point of silicon ($T_{m,Si} = 1685$ K) the linear fit can be expressed by equation:

$$\Delta_f G_T^\circ/(\mathrm{kJ\ mol^{-1}}) = -698.46 + 0.315T/\mathrm{K} \quad (11)$$

where $T > 1685$ K.

A rough estimation of the minimum and maximum values for the $\Delta_f G_T^\circ$ of $MgSiN_2$ was carried out using the following two reactions[31]:

$$2Si_2N_2O + MgSiN_2 = (3/2)Si_3N_4 + (1/2)Mg_2SiO_4 \quad (12)$$

$$(1/2)Si_3N_4 + 2MgO = (1/2)Mg_2SiO_4 + MgSiN_2 \quad (13)$$

Both reactions proceed to the right at temperatures above 1650 K,[7,32,33] consequently the Gibbs free energy of reactions should be negative, resulting in the following conditions:

$$\Delta_f G^\circ(MgSiN_2) > (3/2)\Delta_f G^\circ(Si_3N_4) + (1/2)\Delta_f G^\circ(Mg_2SiO_4) - 2\Delta_f G^\circ(Si_2N_2O) \quad (14)$$

$$\Delta_f G^\circ(MgSiN_2) < (1/2)\Delta_f G^\circ(Si_3N_4) + 2\Delta_f G^\circ(MgO) - (1/2)\Delta_f G^\circ(Mg_2SiO_4) \quad (15)$$

From these conditions the minimum and maximum values for $\Delta_f G^\circ(MgSiN_2)$ were obtained. The thermodynamic data of $\Delta_f G^\circ(Si_2N_2O)$ were taken from Hendry and Fegley,[34–36] the $\Delta_f G^\circ_T$ of other substances from NIST-JANAF tables.[20] The results are shown in Fig. 7, together with the calculated $\Delta_f G^\circ_T$ of $MgSiN_2$ from Eqs. (10) and (11). The Gibbs free energy of formation $\Delta_f G^\circ(MgSiN_2)$ calculated from C°_P is closer to $\Delta_f G^\circ(MgSiN_2)_{min}$.

Finally, it should be pointed out that in the present work the equilibrium conditions have not been attained owing to the flowing nitrogen atmosphere ($1.5\,L\,min^{-1}$) and the obtained data are a rough estimation of the real thermodynamic data.

4. Conclusions

$MgSiN_2$ powder was prepared by direct nitridation of $Si/Mg_2Si/Mg/Si_3N_4$ powder compact in a temperature range of 1350–1420 °C. The oxygen content of $MgSiN_2$ was in the range of 0.4–0.6 wt%. The thermal stability examination showed that $MgSiN_2$ is stable up to 1400 °C at 0.1 MPa N_2 pressure. The activation energy of decomposition calculated from the temperature dependence of weight loss is $\Delta H = 501\,kJ\,mol^{-1}$. The time dependence and nitrogen pressure dependence of $MgSiN_2$ decomposition was also investigated at constant temperature. $MgSiN_2$ is stable at 1560 °C in 0.6 MPa nitrogen atmosphere. Using the experimental data together with the heat capacity published in a literature the Gibbs free energy of formation of $MgSiN_2$ was calculated in a temperature range of (25–2200) °C.

Acknowledgements

Z. Lenčéš acknowledges the financial support by JSPS Japan. Work was supported partly by the Slovak Grant Agencies, projects VEGA 2/0178/10, APVV-0517-07 and LPP-0394/09.

References

1. Buhr H, Müller G, Wiggers H, Aldinger F, Foley P, Roosen A. Phase composition, oxygen content and thermal conductivity of $AlN(Y_2O_3)$ ceramics. *J Am Ceram Soc* 1991;**74**:718–23.
2. Akimune Y, Munakata F, Matsuo K, Hirosaki N, Okamoto Y, Misono K. Raman spectroscopic analysis of structural defects on hot isostatically pressed silicon nitride. *J Ceram Soc Jpn* 1999;**107**:339–42.
3. Watari K. High thermal conductivity non-oxide ceramics. *J Ceram Soc Jpn* 2001;**109**:S7–16.
4. Kitayama M, Hirao K, Tsuge A, Watari K, Toriyama M, Kanzaki S. Thermal conductivity of β-Si_3N_4: II. Effect of lattice oxygen. *J Am Ceram Soc* 2000;**83**:1985–92.
5. Hayashi H, Hirao K, Toriyama M, Kanzaki S, Itatani K. $MgSiN_2$ addition as a means of increasing the thermal conductivity of β-Si_3N_4. *J Am Ceram Soc* 2001;**84**:3060–2.
6. Thompson DP. New post-sintering treatments for improved high-temperature performance Si_3N_4-based ceramics. In: Babini GN, Haviar M, Šajgalík P, editors. *Engineering ceramics' 96: higher reliability through processing*. Dordrecht: Kluwer Academic Publishers; 1997. p. 311–26.
7. Müller R. *Phase stability and thermodynamic calculations in the Mg/Si/N/O system*. PhD. Thesis. Germany: University of Stuttgart; 1981, 32–34.
8. Uchida H, Itatani K, Aizawa M, Howell FS, Kishioka A. Synthesis of magnesium silicon nitride by the nitridation of powders in the magnesium–silicon system. *J Ceram Soc Jpn* 1997;**105**:934–9.
9. Groen WA, Kraan MJ, de With G. Preparation, microstructure and properties of $MgSiN_2$ ceramics. *J Eur Ceram Soc* 1993;**12**:413–20.
10. Lenčéš Z, Hirao K, Kanzaki S, Hoffmann MJ, Šajgalík P. Reaction sintering of fluorine-doped $MgSiN_2$. *J Eur Ceram Soc* 2004;**24**:3367–75.
11. Itatani K, Asoo E, Hayashi H, Hirao K, Koda S. Enhancement of mechanical and thermal properties of $MgSiN_2$ using Si_3N_4. *Silicate Ind* 2004;**69**:275–80.
12. Tanaka S, Itatani K, Hintzen HT, Delsing ACA, Okada I. Effect of silicon nitride addition on the thermal and mechanical properties of magnesium nitride ceramics. *J Eur Ceram Soc* 2004;**24**:2163–8.
13. Hintzen HT, Swaanen P, Metselaar R, Groen WA, Kraan MJ. Hot-pressing of $MgSiN_2$ ceramics. *J Mater Sci Lett* 1994;**13**:1314–6.
14. Davies IJ, Uchida H, Aizawa M, Itatani K. Physical and mechanical properties of hot-pressed magnesium silicon nitride compacts with yttrium oxide addition. *Inorg Mater Jpn* 1999;**6**:40–8.
15. Gaido GK, Dubrovskij GP, Zykov AM. Photoluminescence of europium activated $MgSiN_2$. *Izv Akad Nauk SSSR Neorg Mater* 1974;**10**:564–6.
16. Lenčéš Z, Zhou Y, Benco L, Velič D, Hirao K, Šajgalík P. Electronic structure, thermal and optical properties of magnesium and lanthanum silicon nitrides. In: *Book of abstracts international symposium on new Frontiers of advanced Si-based ceramics and composites*. 2008. p. 38.
17. Kulshreshtha C, Kwak JH, Park YJ, Sohn KS. Photoluminescent and decay behaviours of Mn^{2+} and Ce^{3+} coactivated $MgSiN_2$ phosphors for use in light-emitting-diode applications. *Opt Lett* 2009;**15**(36):794–6.
18. Lenčéš Z, Hirao K, Yamauchi Y, Kanzaki S. Reaction synthesis of magnesium silicon nitride powder. *J Am Ceram Soc* 2003;**86**:1088–93.
19. David J. Study on Mg_3N_2 and some its compounds. *Rev Chim Miner* 1972;**9**:717–35.
20. Chase Jr MW. NIST-JANAF thermochemical tables, fourth edition (part i and part ii). *J Phys Chem Ref Monogr* 1998;**9**.
21. Andrievskii RA, Lyutikov RA. High-temperature dissociation of silicon nitride. *Russ J Phys Chem* 1996;**70**:526–8.
22. Liang J, Topor L, Navrotsky A, Mitomo M. Silicon nitride: enthalpy of formation of the α- and β-polymorphs and the effect of C and O impurities. *J Mater Res* 1999;**14**:1959–68.
23. David J, Laurent Y, Lang J. The structure of $MgSiN_2$ and $MgGeN_2$. *Bull Soc Fr Miner Crystallogr* 1970;**93**:153–9.
24. Kingery WD, Bowen HK, Uhlmann DR. Reactions with and between solids. In: *Introduction to Ceramics*. New York: John Wiley & Sons; 1976. p. 381–447.
25. O'Hare PAG, Tomaszkiewicz I, Seifert H-J. The standard molar enthalpies of formation of α-Si_3N_4 and β-Si_3N_4 by combustion calorimetry in fluorine, and the enthalpy of the α-to-β transition at the temperature 298.15 K. *J Mater Res* 1997;**12**:3203–5.
26. O'Hare PAG, Tomaszkiewicz I, Beck II. CA, Seifert H-J. Thermodynamics of silicon nitride. I. Standard molar enthalpies of formation $\Delta_f H^\circ$ at the temperature 298.15 K of α-Si_3N_4 and β-Si_3N_4. *J Chem Thermodyn* 1999;**31**:303–22.
27. Šesták J, Berggren G. Study of the kinetics of the mechanism of solid-state reactions at increasing temperatures. *Thermochim Acta* 1971;**3**:1–12.
28. Batha HD, Whitney ED. Kinetics and mechanism of the thermal decomposition of Si_3N_4. *J Am Ceram Soc* 1973;**56**:365–9.
29. Jander W. Reactions in solid state at elevated temperatures. *Z Anorg Allg Chem* 1927;**163**:1–30.
30. Bruls RJ, Hintzen HT, de With G, Metselaar R, van Miltenburg JC. The temperature dependence of the Grüneisen parameters of $MgSiN_2$, AlN and β-Si_3N_4. *J Phys Chem Solids* 2001;**62**:783–92.
31. Bruls RJ, Hintzen HT, Metselaar R, van Miltenburg JC. Heat capacity of $MgSiN_2$ between 8 and 800 K. *J Phys Chem B* 1998;**102**:7871–6.
32. Hendry A, Perera DS, Thompson DP, Jack KH. Phase relationships in the MgO–Si_3N_4–Al_2O_3 system. In: Popper P, editor. *Special ceramics 6, Stoke-on-Trent*. UK: British Ceramics Research Association; 1975. p. 321–31.
33. Inomata Y, Yukino K, Matsuyama T, Wada T. Hot-pressing of Si_3N_4 with magnesium compound additives. *Yogyo-Kyokai-Shi* 1976;**84**:534–9.

34. Hendry A. Silicon nitride ceramics. In: Bentzen JJ, Bilde-Sorensen JB, Christiansen N, Horsewell A, Ralph B, editors. *Structural ceramics: processing, microstructure and properties*. Roskilde, Denmark: RISO National Laboratory; 1990. p. 27–38.
35. Fegley MB. The thermodynamic properties of silicon oxynitride. *J Am Ceram Soc* 1981;**64**:C124–6.
36. Kaufman L, Hayes F, Birnie D. Calculation of quasibinary and quasiternary oxynitride systems. *High Temp High Pres* 1982;**14**:619.